X-590-73-273
PREPRINT

NASA TM X-70632

CRUSTAL MOTION MEASUREMENT BY MEANS OF SATELLITE TECHNIQUES

JOSEPH W. SIRY

(NASA-TM-X-70632) CRYSTAL MOTION MEASUREMENT BY MEANS OF SATELLITE TECHNIQUES (NASA) ~~38~~ 42 p HC $5.00 CSCL 08E N74-22965 Unclas G3/13 38486

MAY 1973

GODDARD SPACE FLIGHT CENTER
GREENBELT, MARYLAND

Presented at the
American Geophysical Union
Third GEOP Research Conference
The Ohio State University
May 31 - June 1, 1973

Z

For information concerning availability
of this document contact:

Technical Information Division, Code 250
Goddard Space Flight Center
Greenbelt, Maryland 20771

(Telephone 301-982-4488)

X-590-73-273
Preprint

CRUSTAL MOTION MEASUREMENT BY MEANS OF SATELLITE TECHNIQUES

by

Joseph W. Siry

Presented at the
American Geophysical Union
Third GEOP Research Conference
The Ohio State University
May 31 - June 1, 1973

May 1973

GODDARD SPACE FLIGHT CENTER

Greenbelt, Maryland

CRUSTAL MOTION MEASUREMENT BY MEANS OF SATELLITE TECHNIQUES

by

Joseph W. Siry

ABSTRACT

Crustal motions of the order of several centimeters have been observed to precede earthquakes. Scholz, Sykes and Aggarwal propose a model which relates these and other precursory phenomena to dilatancy. (Scholz, C., Sykes, L., and Aggarwal, Y., "The Physical Basis for Earthquake Prediction," AGU Meeting, Washington, April, 1973.) They present evidence linking the precursor time interval with the earthquake magnitude and the length of the aftershock zone. Dilatant regions of the order of a few tens of kilometers in scale and precursor time intervals ranging from roughly half a year to a year and a half are expected to be of interest in connection with earthquakes of magnitude six, for example. The dilatancy mechanism seems to be operative in the case of thrust faults and probably also in the case of at least some strike-slip events. A system for sensing precursory crustal motions should thus have the capability for determining site positions with an accuracy of the order of a couple of centimeters in a time interval of approximately a quarter of a year at spacings of roughly ten kilometers in a region of interst such as a fault zone. Several hundred such locations are needed to cover the fault systems in the California area.

A system for monitoring such precursory crustal motions is presented. It involves a set of automated corner reflector stations tracked by means of a laser operating in the Geopause satellite. It should be possible to range some three times during every Geopause pass to each of the sites in such an ensemble, weather permitting. One centimeter range data gathered during a quarter of a year should yield position component accuracies of the order of a couple of centimeters. A laser beam of a tenth of a milliradian in diameter would, in general, illuminate a single station in such an array. A broader beam would generate reflections from several sites, yielding overlapping data. A chain or pattern of such overlapping regions can strengthen the solution for site positions. Pressure, temperature and humidity gages can provide refraction correction data. Turnaround transponders interrogated by the Geopause radio tracking system can furnish corresponding data in excessively cloudy regions. This concept offers the prospect of a practical approach to the problem of monitoring precursory crustal motions.

CONTENTS

CRUSTAL MOTION MEASUREMENT BY MEANS OF SATELLITE TECHNIQUES

I. CRUSTAL MOTIONS WHICH ARE PRECURSORY TO EARTHQUAKES

Precursory phenomena of several types have been observed to precede earthquakes. Among these are crustal motions, variations in the ratio of the seismic compressional velocity, V_p, to the seismic shear velocity, V_s, and changes in the electrical resistivity, magnetic fields, radon emission, and the relative numbers of large and small seismic shocks. (Cf. references 1-3.) An example of a vertical crustal motion occurring before a large earthquake is seen in Figure 1. [1,4]

A model which relates these various premonitory effects to dilatancy has been proposed by Scholz, Sykes, and Aggarwal.[1] They present evidence linking the precursor time interval with the magnitude of the subsequent earthquake. This is seen in Figure 2. The long term precursory effects occur months and even years prior to the large earthquakes. They also find a connection between the precursory time interval and the length of the aftershock zone, which is taken as a characteristic dimension. This is exhibited in Figure 3. These data relating a variety of different phenomena are in good agreement with the diffusion relation. This circumstance lends further support to the dilatancy theory as an explanation of the array of effects.

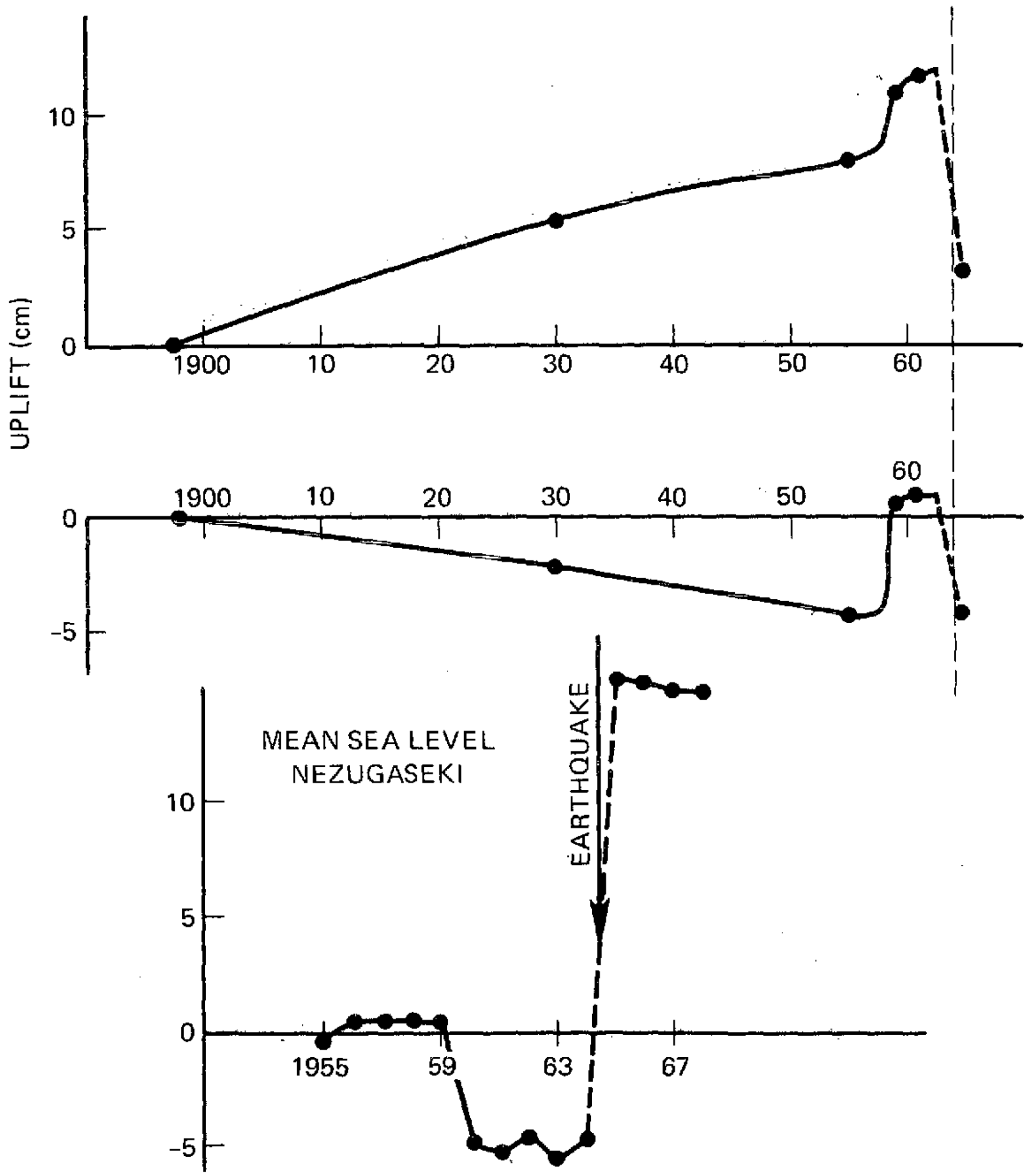

NIIGATA 1964 M=7.5

Figure 1 (References 1 and 4).

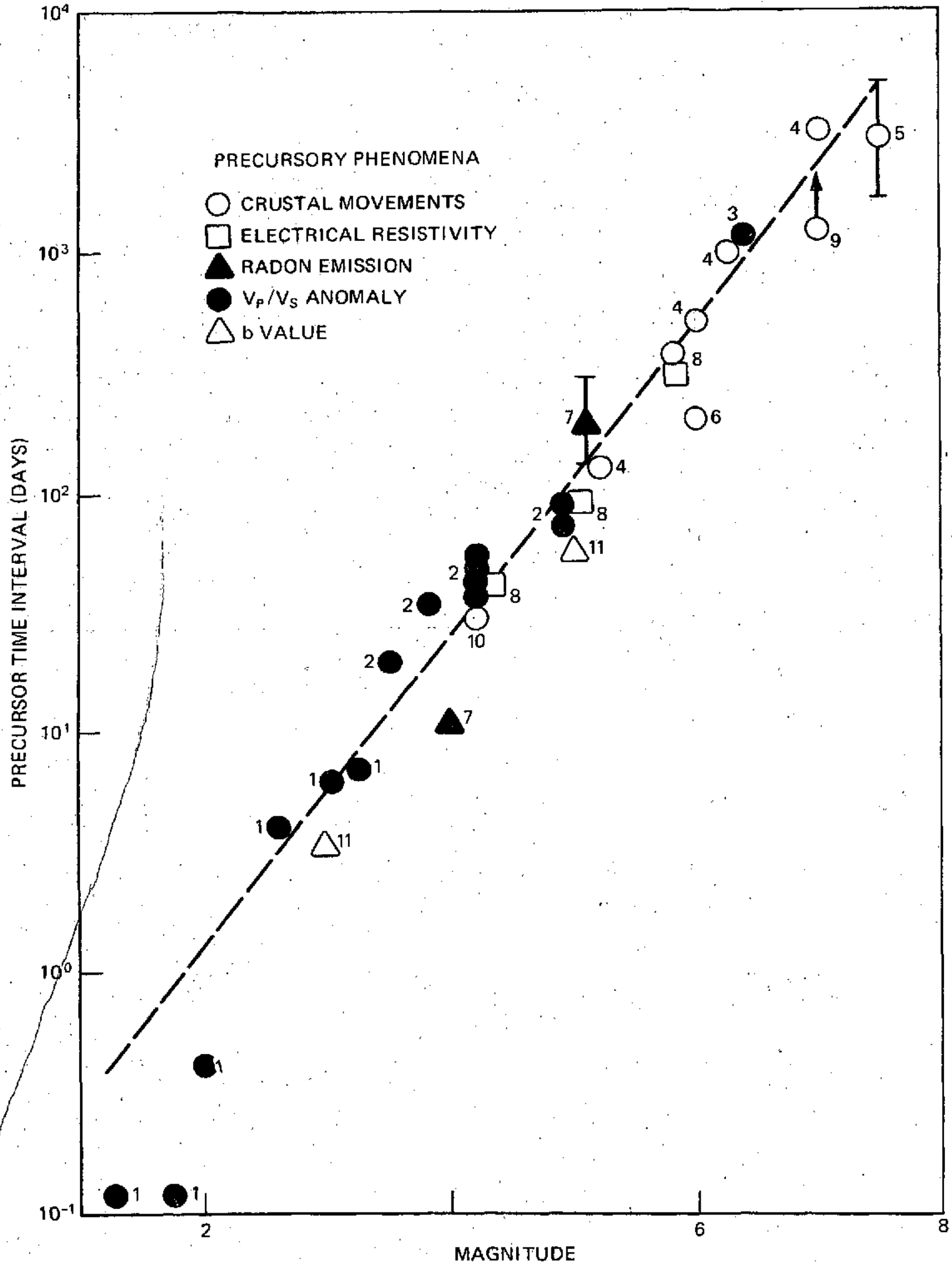

Figure 2 (Reference 1).

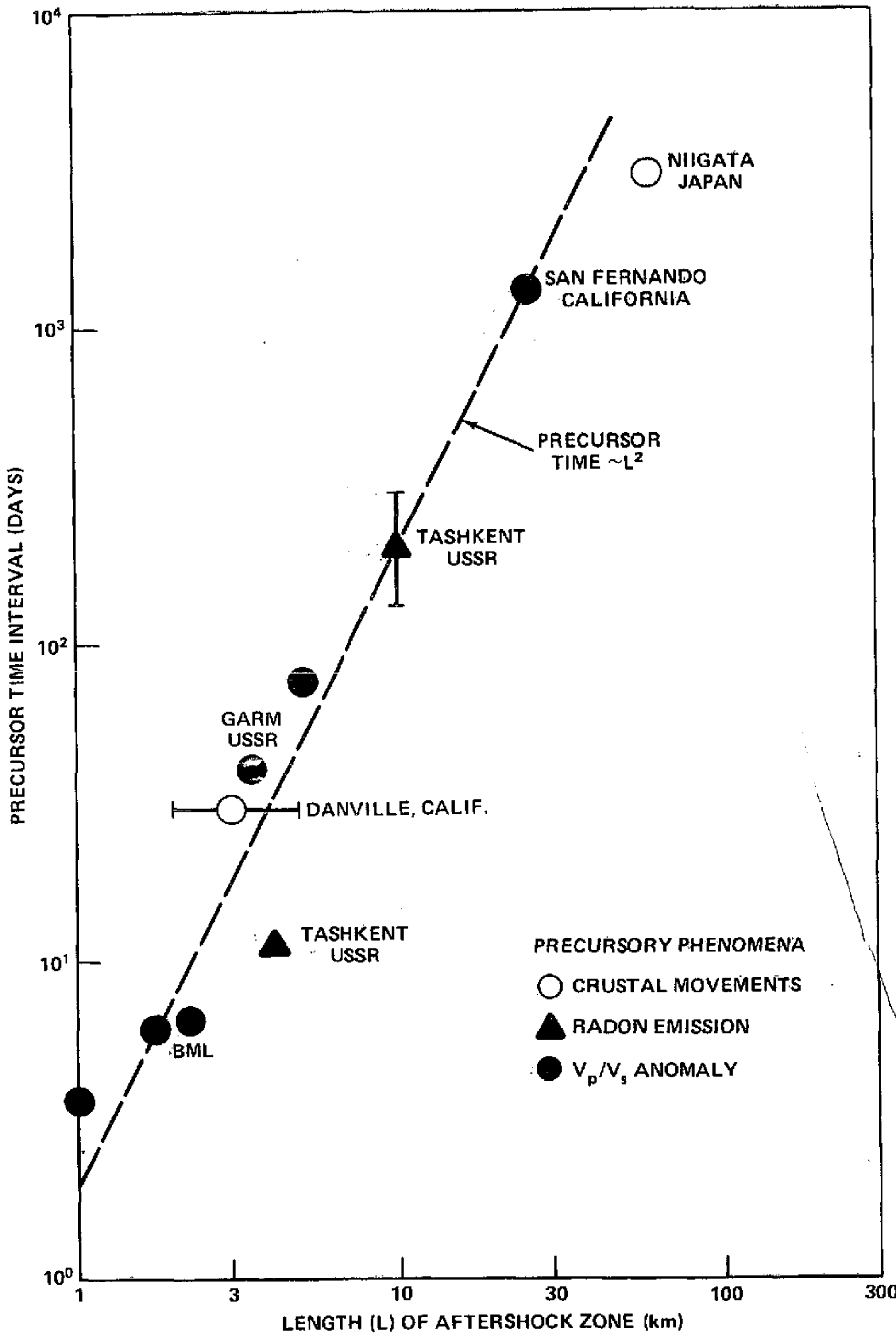

Figure 3 (Reference 1).

The scale of the dilatant region is thus an indicator both of the magnitude of the subsequent earthquake and of the time interval between the earthquake and the precursory phenomena such as crustal motion. The dilatant region itself is about twice the length of the fault or the aftershock zone.

At thrusting faults the vertical precursory crustal motions are of the order of several centimeters. There is also some evidence in connection with the Danville, California earthquake which indicates that it is appropriate to view at least some strike slip events in terms of the dilatancy mechanism. The vertical components of the motion will be approximately a third of the horizontal strain for shallow earthquakes, i.e., ones for which the depth is small relative to the dimensions of the source. This is true for the moderate and large California earthquakes. Scholz, Sykes and Aggarwal point out that, although they cannot demonstrate that premonitory effects occur before shocks deeper than about 10 to 15 km, the depth range where the effect is observed includes virtually all earthquakes on or near the San Andreas fault system in California and most of the world's damaging earthquakes. (1)

Earthquakes of magnitude six or larger can cause significant damage as is pointed out, for example, in Figure 4 which is presented in the NASA Earth and Ocean Physics Applications Program (EOPAP) Plan. (5)

Earthquake	Magnitude	Estimated property damage ($ millions) Contemporary dollars	1966 dollars*	Estimated loss of life
San Francisco, Calif. April 18, 1906	8.3	400	2600	700
Alaska March 27, 1964	8.5	311		114
Long Beach, Calif. March 10, 1933	6.3	50	170	120
Kern County, Calif. July 21, 1952	7.7	50		12
Aleutian Islands April 1, 1946	7.4	25**		173**
Puget Sound, Wash. April 13, 1949	7.0	25		8
Puget Sound, Wash. April 29, 1965	6.5	12		6
Hegben Lake, Mont. August 17, 1959	7.1	11		28
Santa Barbara, Calif. June 29, 1925	6.3	8	26	13
Imperial Valley, Calif. May 18, 1940	7.1	5		9
Montana Series October and November 1935	up to 6.2	4		4
San Fernando, Calif.† February 9, 1971	6.6	553		64

*Based on Engineering News-Record Building Cost Index.
**Most of the damage and loss of life resulted from the tsunami that hit the Hawaiian Islands.
†The San Fernando, California, earthquake of February 9, 1971, Geological Survey Professional Paper 733, U.S. Government Printing Office, 1971.

Figure 4. Property Damage and Loss of Life from Major Earthquakes in the United States in the Present Century.

II. PRELIMINARY DESIGN PARAMETERS FOR A PRECURSORY CRUSTAL MOTION AND REGIONAL STRAIN FIELD MONITORING NETWORK

A. Crustal Motion Characteristics of the Dilatancy Model with Particular Reference to Major Earthquakes

A magnitude six earthquake can be characterized in an order of magnitude way in terms of the preceding discussion as one associated with a dilatancy which precedes the earthquake by a time interval of the order of half a year to a year and a half, and a dilatant region some 20 to 30 kilometers long which is marked by crustal motions having a scale of several centimeters in the case of thrusting faults and at least some strike-slip faults. (Cf. Figure 5.)

A system for monitoring such precursory crustal motions can be an important element of an earthquake prediction capability. Such a system would involve an array of stations about 5 to 10 km apart along the fault deployed in two lines symmetrically placed on each side of it and separated by a distance comparable to the interval between the sites in each line. This arrangement is indicated in Figure 6. This means an average of one site for roughly every four kilometers of fault line. Position components should be measured to the order of a centimeter or two in times of approximately a quarter of a year or less.

B. The California Region Viewed from the Standpoint of Possible Criteria for Predicting Earthquake Locations

An extensive study of possible criteria for predicting earthquake locations has been conducted by Kelleher, Sykes and Oliver. [3] They have categorized

A Magnitude 6 Earthquake can be Characterized in an Order of Magnitude Way as Follows:

Precursor Time Interval:	0.5 - 1.5 yr
Fault Length:	10 - 15 km
Dilantant Region Length:	20 - 30 km

Crustal Motion in Dilatant Region:

At Thrusting Fault - Several cm Vertical Motion

At Strike Slip Fault - Vertical Motion ~ 1/3 Horizontal Motion

Scale of Dilatant Region is an indicator of Time and Magnitude of Subsequent Earthquake

Figure 5.

segments of the circum-Pacific belt in terms of the following initial set of criteria.

"1. The segment is a part of a major shallow seismic belt characterized predominantly by strike slip or thrust faulting (plate boundaries other than spreading ridges according to plate tectonic theory).

"2. The segment has not ruptured for at least 30 years."(3)

The shallow seismic belts which they studied here, i.e., those which satisfy the first of these criteria, are indicated in Figure 7a. The segments which

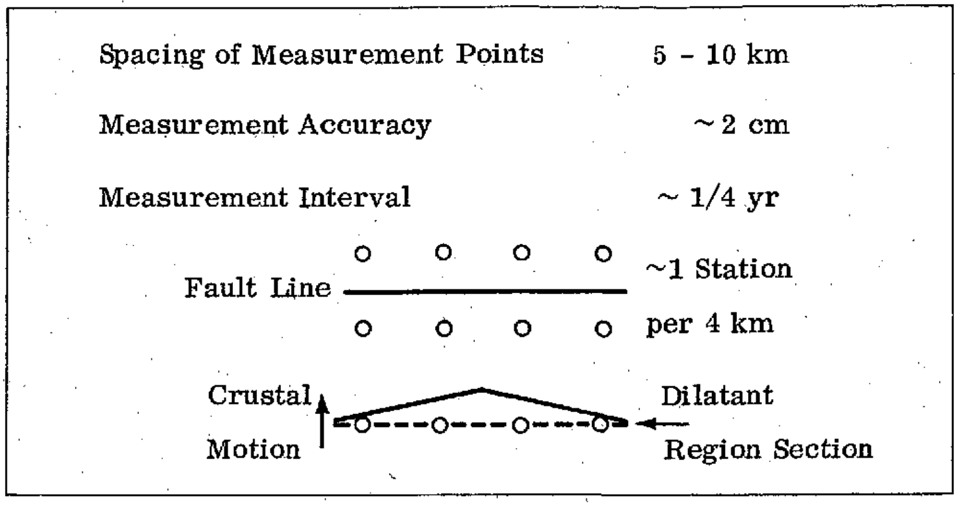

Figure 6. Precursor Crustal Motion Monitoring Network for Major Earthquakes, i.e., M $\geqq$ 6 Preliminary Design Parameters

meet both of the initial criteria and hence are designated by them as areas of 'special seismic potential' are indicated in Figure 7b.[3]

Interest in certain of these latter segments of special seismic potential is further heightened if at least one of the following three criteria is fulfilled.

"1. A historic record of one or more large earthquakes along a segment is taken as evidence that large earthquakes can again occur along that segment. This criterion is not trivial since several segments along the major plate boundaries examined in this study are not known to have experienced large earthquakes during historic times.

"2. Evidence based on historical data and relative plate motions suggests that the recurrence interval for large earthquakes is near the duration

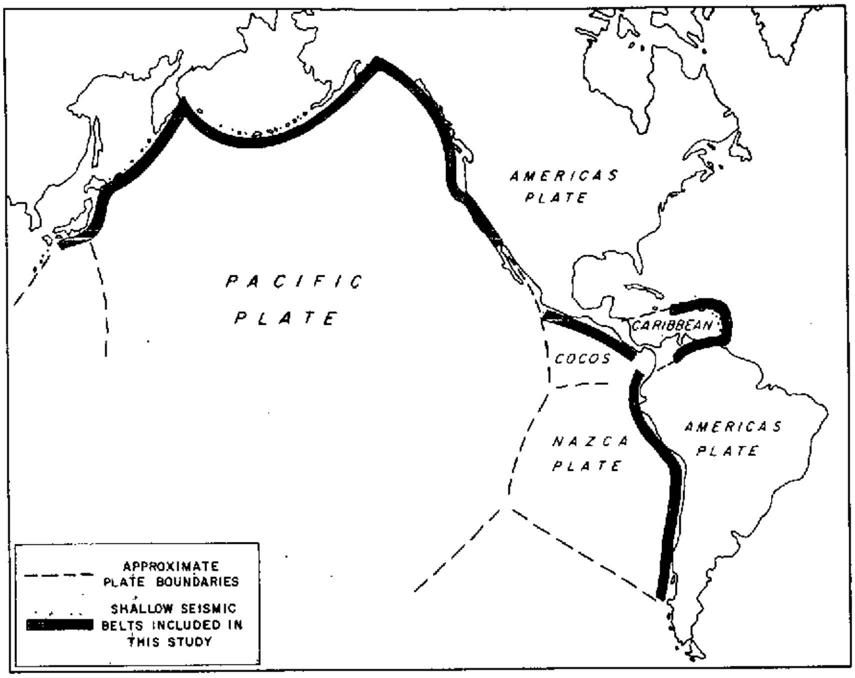

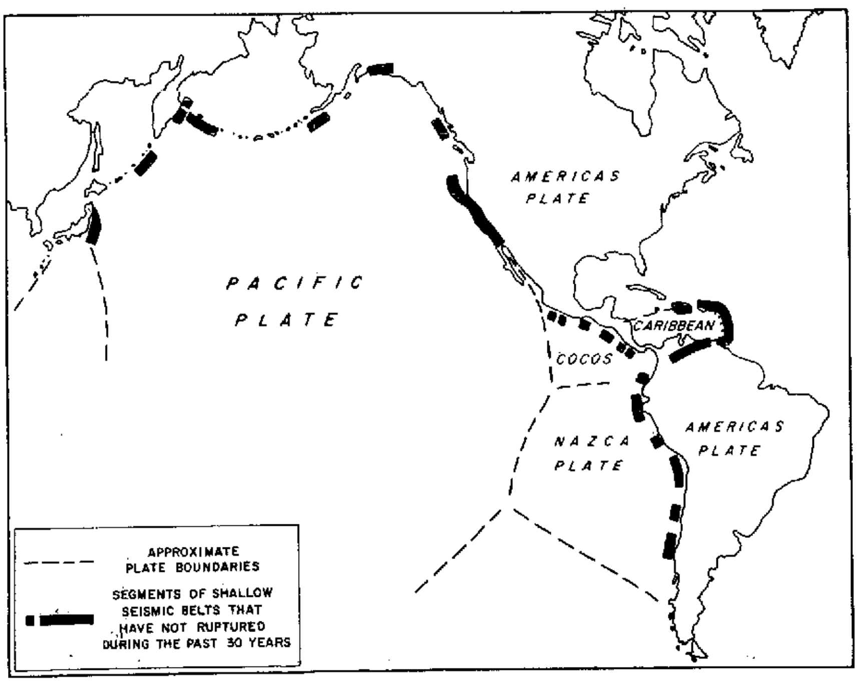

Figure 7a. (Top) Major shallow seismic belts examined by Kelleher, Sykes and Oliver. (3)

Figure 7b. (Bottom) Shallow seismic zones of Figure 7a with rupture zones of the past 30 years removed. Zones of sea floor spreading also removed. (3)

of the time interval since the most recent large earthquake of that segment.

"3. The segment appears to be the site for the next event of a series of earthquakes progressing regularly in space and time."[3]

Areas of special seismic potential which meet at least one of these 3 criteria are shaded doubly in Figure 8. Looking more closely at a small part of this region, they find the picture of the San Andreas fault system which is seen in Figure 9, where the shading conventions are the same as in the previous figure. Added in Figure 9 are indications of the zones of the great earthquakes of 1857 and 1906.[3]

Allen views the San Andreas fault system as being composed of five segments for the purpose of estimating the potential for future great earthquakes.[3,6] He proposed that the 1857 and 1906 earthquake zones are probable locations for infrequent great earthquakes and that the three other segments of the San Andreas system release strain energy by means of creep and small- and moderate-magnitude earthquakes more or less continuously and hence are not likely locales for great earthquakes.[3,6] Significantly, however, Scholz, Molnar and Johnson found in the laboratory that a small amount of stable slip always precedes stick slip.[3,7] It is of interest to note in this connection that the Imperial Valley neighborhood southeast of the 1857 break is an area where strain may be accumulting even though the region is active, as is indicated in

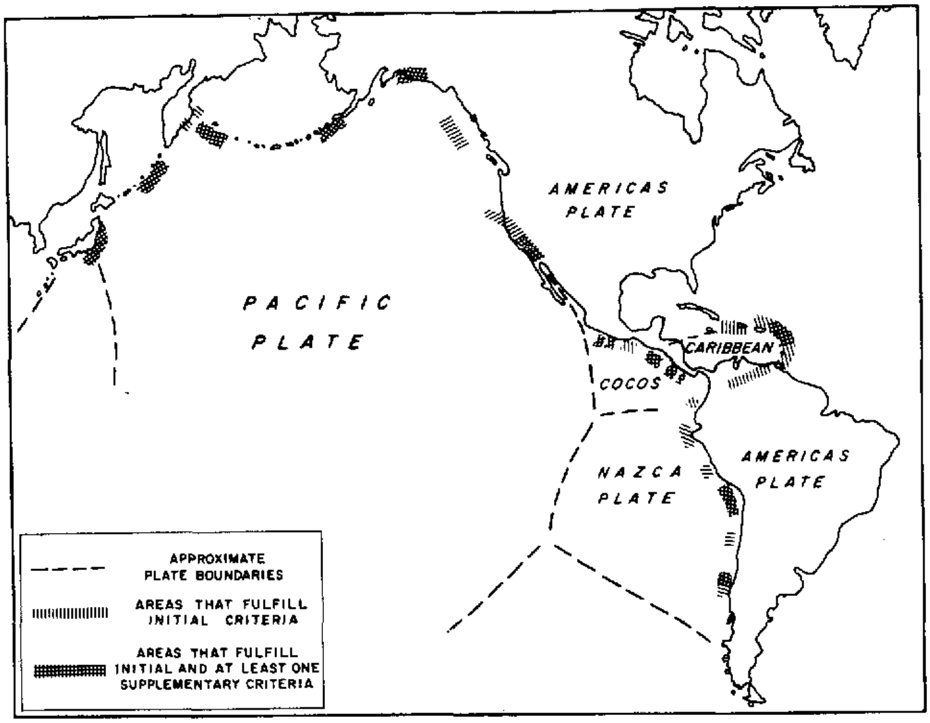

Figure 8. A summary of segments and plate boundaries that fulfill the criteria of Kelleher, Sykes and Oliver for identifying likely locations for large earthquakes of the near future.[3] All areas that meet these criteria are designated regions of special seismic potential. Because of the scale, the areas indicated are approximate. See reference 3 for detailed descriptions and qualifications.

Figure 10. Similarly, fault creep slippage along the San Andreas is widespread between the 1857 and 1906 earthquake zones, yet the question as to whether strain is accumulating or is already high there is a controversial one.[3, 8-13] Kelleher, Sykes and Oliver point out that special interest must be attached to creeping segments of the San Andreas if creep at active faults indicates high stress.[3] They point, too, to the region southeast of the 1857 earthquake zone as also being of special interest since it has not broken during historic time. Conspicously high apparent stresses from earthquakes in the area between San

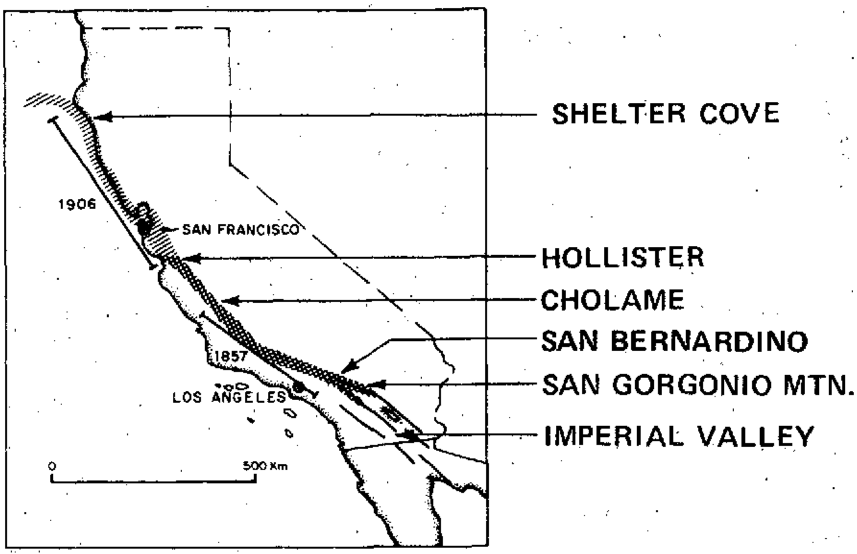

Figure 9. Segments of the San Andreas system that fulfill initial or supplementary criteria of Kelleher, Sykes and Oliver.(3)

Bernardino and the San Gorgonio mountain were observed by Wyss and Brune.(3,14) The locations of major earthquakes occurring in eastern California and western Nevada including, for example, the Owens Valley earthquake of 1872 are also seen in Figure 10. The segment of the San Andreas fault system having special seismic potential is some 1100 kilometers long as can be seen in Figure 9. The zones of the 1857 and 1906 earthquakes, which are probable locations for future great earthquakes, and hence are of particular interest from the standpoint of the present discussion, are together nearly 800 kilometers long. The San Andreas fault system as a whole is some 1400 kilometers long.

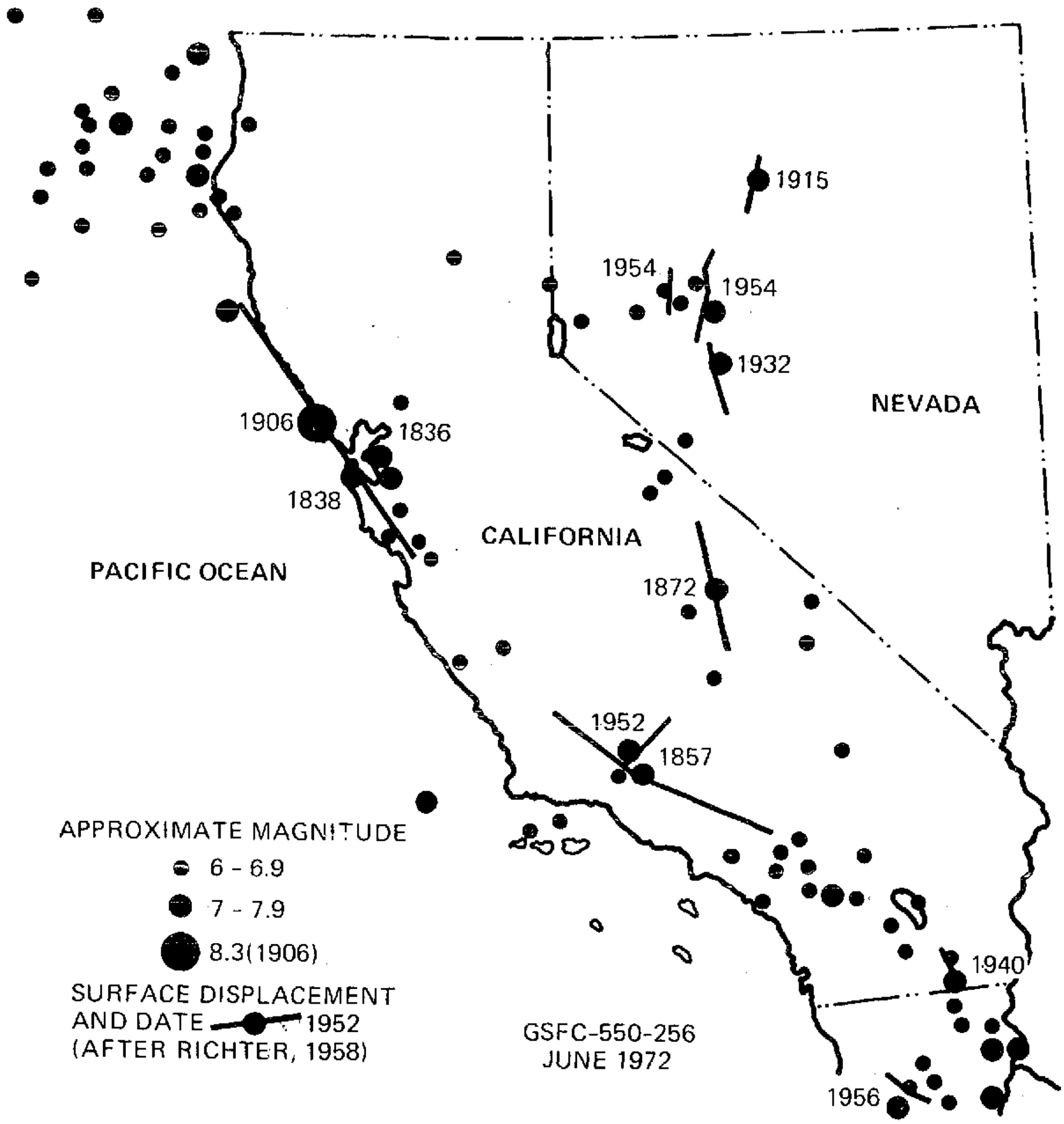

Figure 10. Major Earthquakes Along the Fault

C. A Regional Strain Field Monitoring Network

Kelleher, Sykes and Oliver call attention to the clear need for surveys across faults which are parallel to the Cholame-Hollister fault zone but many tens of kilometers from it.[3]

The measurement of regional strain fields is contemplated in the NASA EOPAP Plan.[5] In California, some of the arrays for this purpose would be roughly normal to the San Andreas fault line at spacings of, e.g., 10, 30, 100, 300, and perhaps 1000 km, say. There would be at least several such lines on each side of the fault, to the extent that land and island geography permits.

As the preceding discussion indicated, it will probably be of interest to locate such lines near the ends and centers of the 1857 and 1906 earthquake zones, and also north of Shelter Cove, between Cholame and Hollister, and one or more southeast of San Bernardino, e.g., in the Imperial Valley Region, and perhaps south of it. Such locations are indicated schematically in Figure 11.

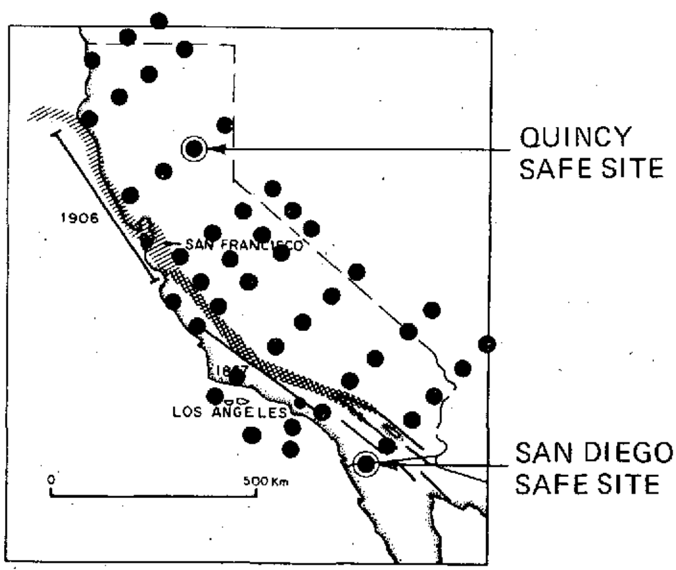

Figure 11. The San Andreas fault system as depicted by Kelleher, Sykes and Oliver.[3] Added are schematic possible locations for regional strain field measurement sites. The locations of the present SAFE sites near Quincy and San Diego are also shown.

The San Andreas Fault Experiment (SAFE) constitutes the first step in the NASA EOPAP regional strain field measurement program.[5, 23-25] The SAFE Project is aimed at determining the changing distance between mobile laser stations near Quincy and San Diego in California. The locations of these two sites are also indicated in Figure 11. Data obtained through laser tracking of existing satellites such as Beacon Explorer-C will be used for the initial intersite distance determinations.

D. The Precursory Crustal Motion and Regional Strain Field Monitoring Network

The regions of interest in Figures 9 and 10, in all, have a linear extent of the order of a quarter to half on earth's radius. This corresponds to some 400 to 800 stations.

The preliminary design parameters for a premonitory crustal motion and regional strain field measurement network system presented in this section do indeed pose formidable problems which arise chiefly due to the stringent accuracy requirements associated with station location determination and the extremely large number of sites involved.

III. A PRECURSORY CRUSTAL MOTION AND REGIONAL STRAIN FIELD MONITORING SYSTEM

A. General Characteristics

It is proposed to establish a precursory crustal motion and regional strain field monitoring system by placing corner reflectors at the sites indicated in the preceding discussion and tracking them by means of a laser system operating in the Geopause satellite.[15] Each of the automated ground stations would also be equipped with simple apparatus for measuring atmospheric pressures, temperatures and humidities, and telemetering them via Geopause. Sites troubled by excessive cloudiness would also be equipped with turnaround transponders operating in conjunction with the Geopause radio tracking system. Such a Precursory Crustal Motion and Regional Strain Field Monitoring System is indicated schematically in Figure 12.

In this approach, the problems associated with the site location accuracies are attacked by means of the Geopause spacecraft equipped with accurate laser and radio range tracking systems, and the challenge posed by the very large number of sites is met by means of the relatively simple and inexpensive automated ground stations.

B. The Geopause Spacecraft

The state of the art of orbit analysis and station position determination is roughly an order of magnitude away from the accuracy levels required for this precursory crustal motion application. The realization of the required accuracies awaits the solution of four kinds of problems, namely, those involving orbit determination and the lack of sufficient knowledge of tracking system biases, the gravity field and tracking station locations.

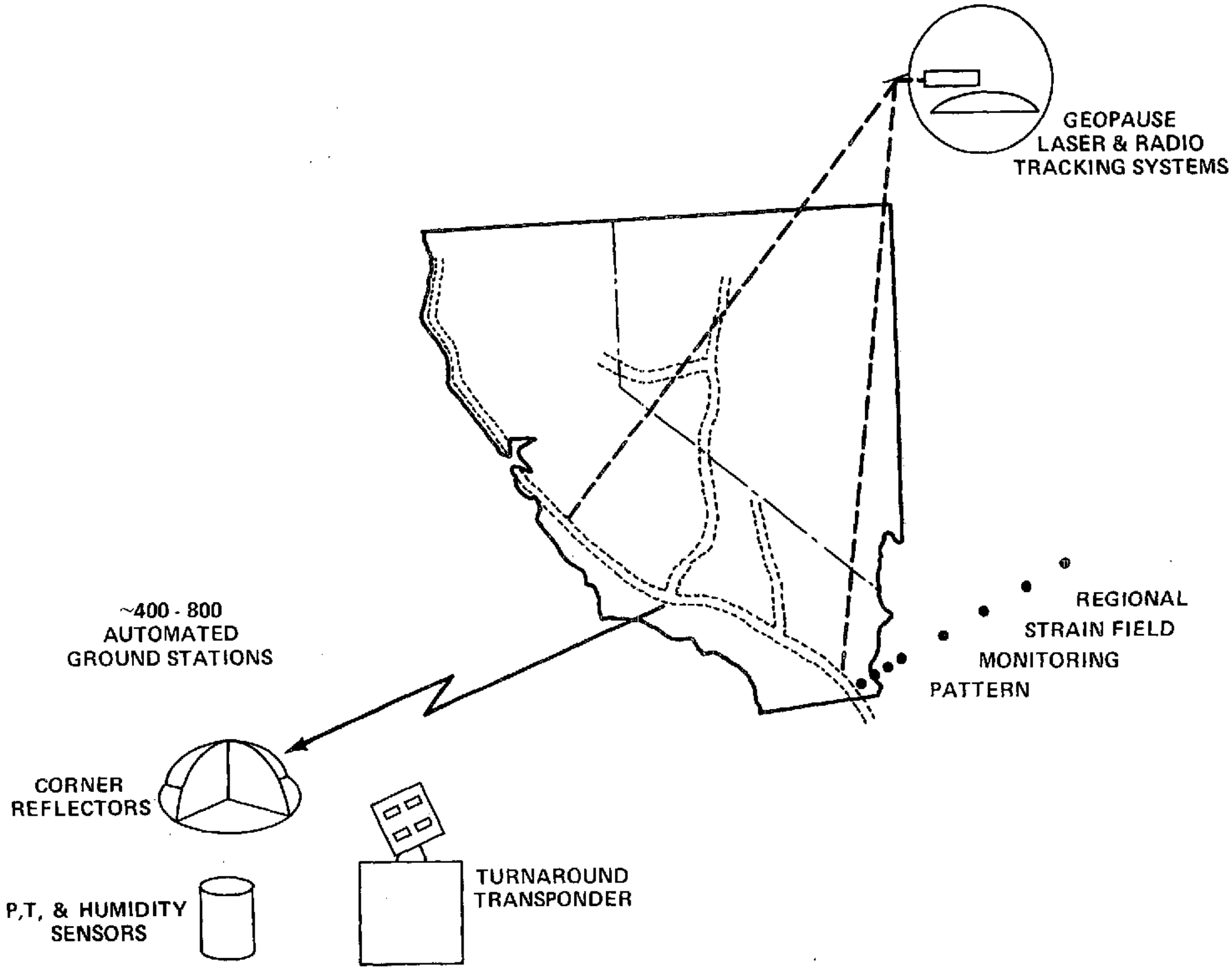

Figure 12. Precursory Crustal Motion & Regional Strain Field Monitoring System Based on the GEOPAUSE Satellite

The Geopause satellite system concept offers promising approaches in connection with all of these areas.[15] A typical Geopause satellite orbit has a 14 hour period, a mean height of about 4.6 earth radii, and is nearly circular, polar, and normal to the ecliptic. At this height only a relatively few gravity terms have uncertainties corresponding to orbital perturbations above the decimeter level. (Cf. Figure 13.) The orbit is, in this sense, at the geopotential boundary, i.e., the "geopause." The few remaining environmental quantities which may be significant can be handled by means of orbit analyses and surface force compensation systems or accelerometers.

The Geopause satellite system also provides the tracking geometry and coverage needed for determining the orbit, the tracking system biases and the station locations. This is indicated in Figures 13 and 14.

Results of an analysis based on a week of simulated observations from ten NASA affiliated sites are shown in Figure 15. It was assumed that range data having a two centimeter bias were taken at intervals of a quarter of a minute. The uncertainties in the geopotential coefficients were taken to be a quarter of the difference between the SAO 1969 Standard Earth Model and the APL 3.5 Model.[16-18] This assumption has been found to be consistent with some observational experience.[18] The quantities solved for were the station position coordinates, GM and the sets of geopotential coefficients listed in Figure 15. The resulting uncertainties in these quantities are also shown there.

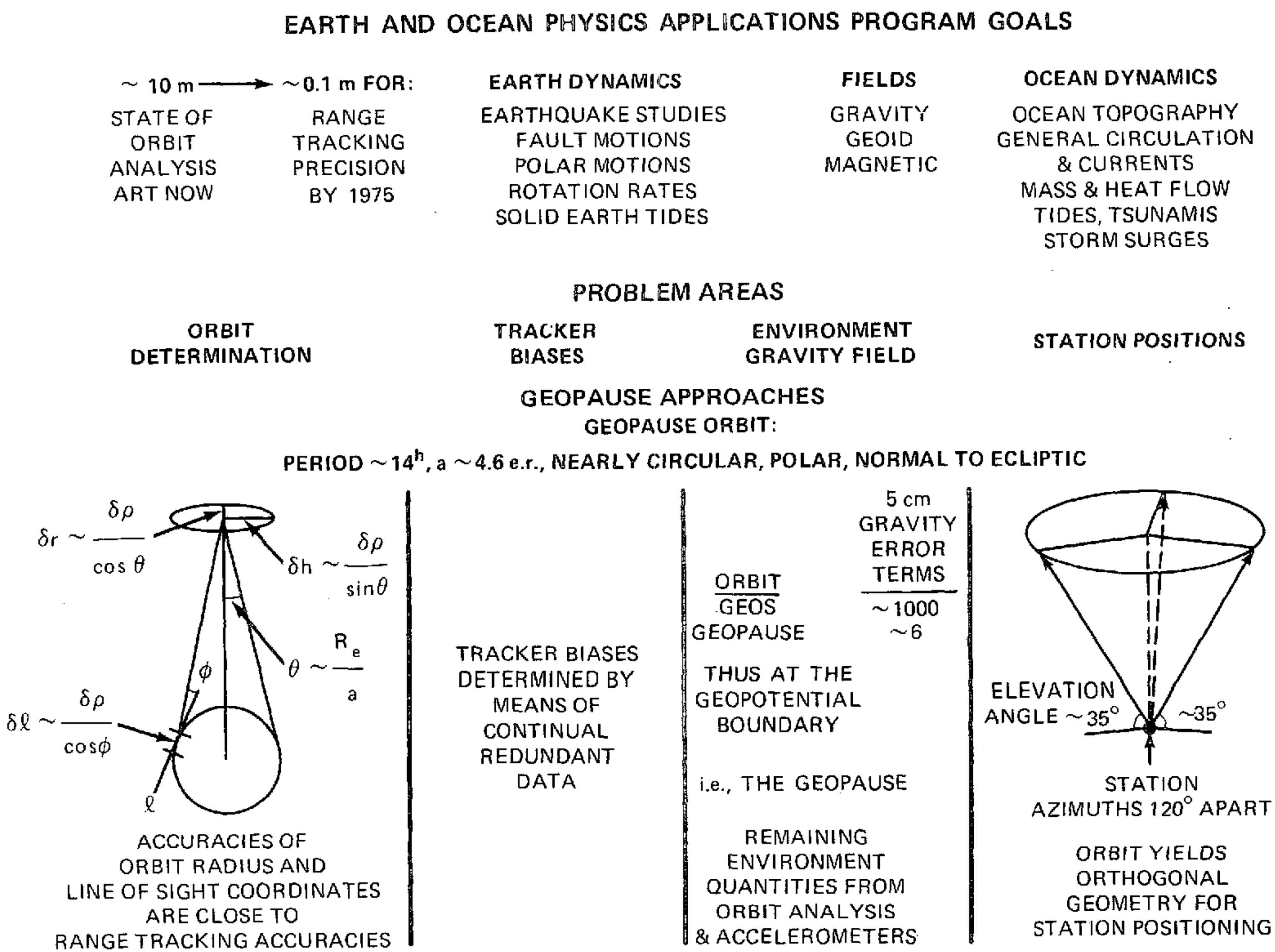

Figure 13. GEOPAUSE Approaches to the Meeting of Earth and Ocean Physics Applications Program Goals

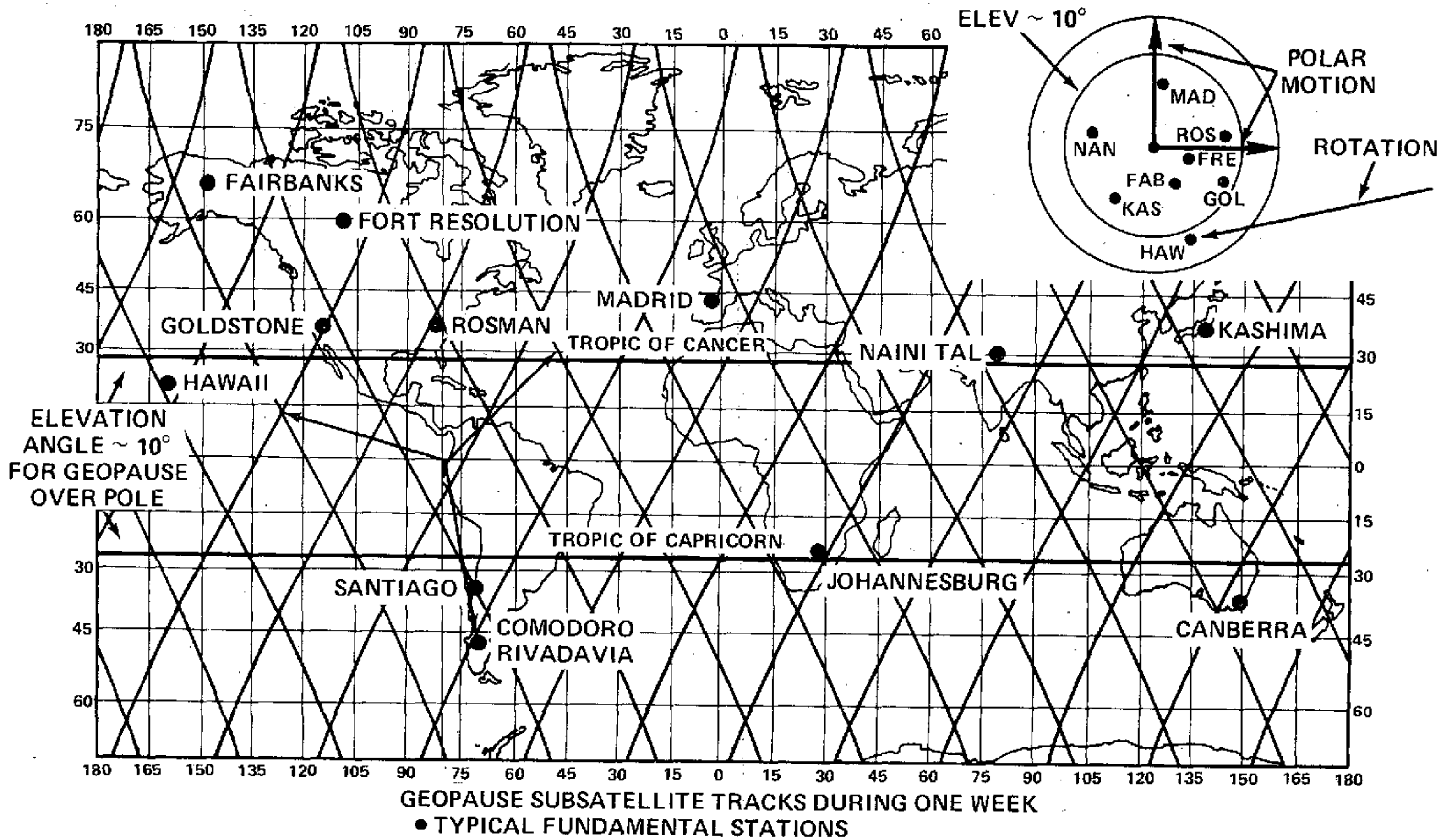

Figure 14. Geopause Orbit Yields the Geometry for Determination of Orbit, Tracker Biases, GM, Station Locations, Fault Motions, Polar Motions, Rotation Rates, Tides

Adjusted Parameter	Standard Deviation ($\times 10^{10}$)	Adjusted Parameter	Standard Deviation (mm)	Adjusted Parameter	Standard Deviation (mm)
GM	9	ROSMAN X	5	JOHANNESBURG X	31
C(2, 2)	2	ROSMAN Y	34	JOHANNESBURG Y	40
S(2, 2)	35	ROSMAN Z	39	JOHANNESBURG Z	35
C(3, 1)	270	SANTIAGO X	3	KASHIMA X	26
S(3, 1)	140	SANTIAGO Y	37	KASHIMA Y	33
C(3, 2)	5	SANTIAGO Z	40	KASHIMA Z	41
S(3, 2)	5	ROSMAN-L Y	33	CANBERRA X	7
C(3, 3)	7	ROSMAN-L Z	39	CANBERRA Y	45
S(3, 3)	1	GOLDSTONE X	20	CANBERRA Z	38
C(4, 2)	21	GOLDSTONE Y	33	FAIRBANKS X	4
S(4, 2)	160	GOLDSTONE Z	39	FAIRBANKS Y	20
C(4, 3)	1	COMODORO RIVADAVIA X	5	FAIRBANKS Z	48
S(4, 3)	3	COMODORO RIVADAVIA Y	30	HAWAII X	9
C(4, 4)	0.1	COMODORO RIVADAVIA Z	45	HAWAII Y	37
S(4, 4)	2	MADRID X	19	HAWAII Z	38
		MADRID Y	32		
		MADRID Z	41		

Assumptions: Range bias, 2 cm. Range rate bias, 0.05 mm/s. Geopotential Harmonic Coefficient Uncertainties, 0.25 (SAO M1-APL 3.5). Tracking Interval, 1 week. Rms and mean of magnitudes of station coordinate standard deviations are 3.1 and 2.7 cm, respectively.

Figure 15. Geopause Satellite Orbit Properties-Determination of Gravitational Parameters and Coordinates for Stations of a Typical Fundamental Network

The designation "Rosman L" denotes a site whose longitude was effectively fixed and taken to be 90° W for reasons of convenience associated with the program. The study was carried out using the program system employed in connection with the analyses of references 15 and 18. The uncertainties in the station coordinates obtained in this case are listed in Figure 15. The largest is 4.8 centimeters. The root mean square value and the mean value of the magnitudes are 3.1 and 2.7 centimeters, respectively.

Since the Geopause spacecraft will be simultaneously visible from four or more sites in several parts of its orbit, it will become practical to determine tracking instrument biases on a continuing basis. For example, when Geopause is over the North Pole, it is visible at elevation angles above about ten degrees not only from the arctic zone but also from the entire temperate zone, i.e., from all stations north of the Tropic of Cancer. This includes most of the Northern Hemisphere stations affiliated with NASA. Similar remarks apply to the visibility of Geopause when it is over the South Pole or near the equatorial plane. This visibility of Geopause over very wide zones of the earth not only means that tracking system biases can be determined on a regular continuing basis, but also that the effects of the earth's polar motions and rotational rate variations can also be observed frequently. Accordingly, it will be possible to decrease correspondingly the adverse effects of these factors on the accuracy of site position determinations.

It is anticipated that it will also be helpful to include as fundamental stations some locations in regions of relative crustal stability such as a Canadian shield site at Fort Resolution, for example.

The analysis summarized in Figure 15 was based on tracking data obtained during a single week, which is the basic time interval during which a geometrically strong set of data can be obtained with Geopause for all stations over the globe. Much of the geometrical strength of the result is obtained from the three normal place observations during each pass which occur on the rising and setting branches and near culmination.

The Geopause satellite will be visible from a point or a region such as California for about five hours during a nearly overhead pass. If, say, five seconds are allowed for both the ranging to a ground site and the pointing motion to the next site, there would be enough time during a nearly overhead pass to make a total of some 3000 site observations, or 3 or more observations per site.

Laser beams having a diameter of some 20 arc seconds corresponding to a spot size at the ground of 3 to 6 km are practical. Such a beam would, in general, illuminate a single site. Somewhat broader beams of 15 or 20 km spot size would generate reflections from several sites, yielding overlapping data. A chain or pattern of such overlapping data sets would strengthen the solution for the site positions in general, and the relative site positions in particular.

The different returns could, in general, be easily distinguished on the basis of prior knowledge of the ranges. The latter would usually differ by kilometers, while knowledge of the positions of the sites and of the Geopause satellite would be orders of magnitude smaller than this, i.e., of the order of less than a meter. The information which could be generated on the basis of the range predictions could be used, say, to program range gates.

It also appears that it will be feasible to maintain knowledge of the Geopause attitude with adequate adequacy, i.e., of the order of 5 to 10 arc seconds, and hence to control or point the laser mirror beam correspondingly. (Cf., for example, reference 19.)

Programs for pointing the laser to the numerous targets could be generated in a ground-based computer and transmitted to the Geopause control system computer. The laser system might alternately range to a site and then move to the next one. On the other hand, it might simply move continuously at a slowly varying or infrequently changing rate, ranging to the sites in a linear array at the appropriate times as it passes them.[20] In either case, the pointing motions and rates involved are reasonable. Thus it appears that during nearly overhead Geopause passes, it will be technically feasible from the standpoint of controls and pointing to obtain three normal places, each based on several individual measures, for each of the hundreds of sites in a regional network such as the California-Nevada one contemplated in Figure 12. Power resources of a specific

Geopause design will govern the rate at which data would be gathered. It appears that this point will probably not be a critical one, however, since it is estimated that the time available for determining the site positions is an order of magnitude or more longer than the basic one week interval during which Geopause affords the opportunity for complete geometrical coverage.

Experience indicates that the data set actually required to achieve a given result may be larger than that implied by an analysis such as the one described above in connection with Figure 15. This may be due, in part at least, to the fact that weather and other practical factors tend to increase the amount of time which is needed to achieve a geometrically strong data set. Even so, it seems that a reasonable margin is available here.

The Geopause radio tracking system will, in general, interrogate more than one transponder if several neighboring sites are equipped with them. The remarks made above in connection with laser ranging concerning the ability to distinguish between the various returns apply here too. Control and pointing capabilities needed for the laser system are more than adequate for the radio system.

C. The Automated Ground Stations

The automated ground stations would include laser retro-reflector arrays, meteorological sensors and, as appropriate, radio turnaround transponders.

Four corner reflectors in a Cartesian array would provide the hemispherical coverage. These would be suitably mounted on rock formations or occasionally on concrete piers. A transparent cover could be hemispherical, or consist simply of four face planes perhaps at a fairly steep angle forming a spire. It could be kept sufficiently clear by wipers and/or a blower. Power could be furnished by batteries which might be powered by solar cells if experience indicates such an approach to be cost effective. Servicing of non-responding sites and periodic maintenance, battery replacement, etc. could be accomplished by truck and helicopter patrols. Fencing may be useful in some cases to discourage souvenir hunters. Additional meteorological ground stations forming a larger linear array with roughly 20 km separations straddling the basic sites would provide a two-dimensional data base for refraction corrections. Laser corner reflectors and turnaround transponders at such outlying sites could provide additional data concerning fault motions having a corresponding scale. The dilatant regions may not extend out to these distances very often.[21] Accordingly, if reflectors and transponders were placed at such sites, they would serve primarily to provide some additional information about regional strain fields.

The turnaround transponders would be, in general, of the type which are already being readied in connection with the ATS-Nimbus satellite-to-satellite tracking (SST) experiment and the SMS tracking system. The antenna, for example, could be of moderate size and gain, comparable to the Nimbus SST transponder antenna, for example. This would provide the necessary link margins, and yet not place excessively stringent requirements on the pointing control system. Antennas with a beam width of the order of a tenth of a radian or so would need to be repointed only every minute or even only once every several minutes in order to follow the relatively slow motion of Geopause as it is seen from a ground station. Commands to point the turnaround transponder antennas would come from Geopause. The turnaround transponder sites would also be equipped with radiometers for gauging the water vapor contribution to the refraction correction where this is necessary. Geopause laser and radio tracking systems should be able to provide ranging data with an accuracy of the order of a centimeter once the refraction correction data are applied. (Cf. for example, refer- cnce 22.)

Characteristics of the Precursory Crustal Motion and Regional Strain Field Monitoring System are summarized in Figure 16.

Once the warning is given and the dilatant region has been located with this system, other equipment can be brought to bear on the problem. For example, seismic velocity measurements can be used to trace out the history of the V_p/V_s curve. Resistivity measurements might also be made. Data gathered by means of the various additional techniques would generate further confidence in the earthquake predictions.

The cost of an automated ground station may turn out to be of a lower order than the cost of preparing a site for a mobile ground station.

Geopause Range Tracking Systems	Automated Ground Stations
Laser System 0.1 - 0.2 mil beam, 2-8 km spot size 6" attitude control Range to: ~ 720 sites/hr ~ 3000 sites/overhead pass ~ 3 ranges/site/overhead pass ~ 2 cm position component accuracy in 1/4 yr Radio System Multiple return discrimination via programmed range gates ~ 2 cm position component accuracy in 1/4 yr Laser & radio systems also track Low-altitude spacecraft yielding Oceanographic and gravity data	Laser Corner Reflector Stations 4 large open corner reflectors in Cartesian array Rock mounting or concrete pier Hemispherical or spire transparent cover-wipers/blower P, T, & humidity gages at corner reflector sites and at peripheral sites for 2-dimensional data measures relayed through Geopause Batteries/solar cells - fencing if needed Truck and helicopter maintenance patrols servicing non-responding sites and for periodic maintenance, battery replacement, etc. Radio Turnaround Transponder Stations Added at low visibility sites, e.g., under persistent fog or clouds, etc. Commands from Geopause for antenna pointing, etc. Radiometer for water vapor refraction correction

Figure 16. Precursory Crustal Motion Monitoring System

The Geopause laser and radio tracking systems would also be used to track the low-altitude Earth and Ocean Physics Applications Program spacecraft yielding oceanographic and gravity data. (Cf. references 5, 15, and 23.)

Some conventional laser, VLBI, and radio ground stations of the type already planned will still be needed as part of the overall Geopause system in connection, for example, with the determination of its orbit and the validation and calibration of the Geopause tracking systems. (Cf. Figure 14, for example.)

The concept outlined here based on geopause satellite techniques offers the prospect of a practical approach to the problem of monitoring secular variations in positions such as precursory crustal motions and regional strain fields and providing data useful for earthquake predictions.

The above discussion is in terms of the California region. Similar approaches might be applied in some of the other areas shown in Figures 7 and 8, and in other parts of the world indicated in Figure 17 which are troubled by seismicity such as the Middle East, to the extent that geography and other factors allow.

Areas of high seismic risk in central and eastern North America indicated in Figure 18 may also be of interest from the standpoint of crustal motion measurement.

It is a pleasure to acknowledge helpful discussions with Drs. C. Scholz, F. Vonbun, H. Plotkin, and D. Smith, and Messrs. H. Hoffman, S. Kant, P. Minott, P. Schmid, and S. Stevens.

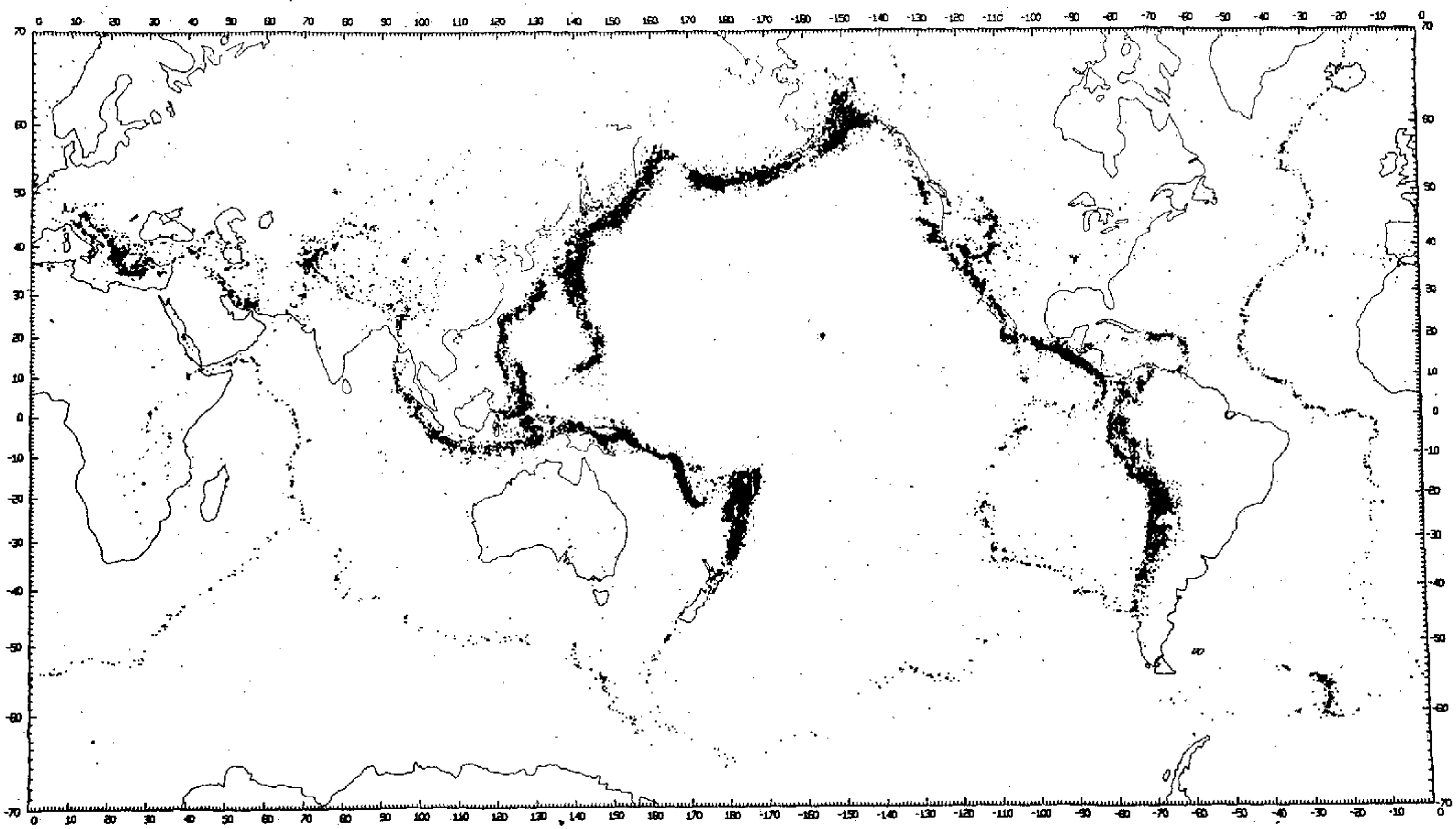

Figure 17. Seismicity of the earth, 1961-1967. Depths to 700 km. Refs. 3, 26.

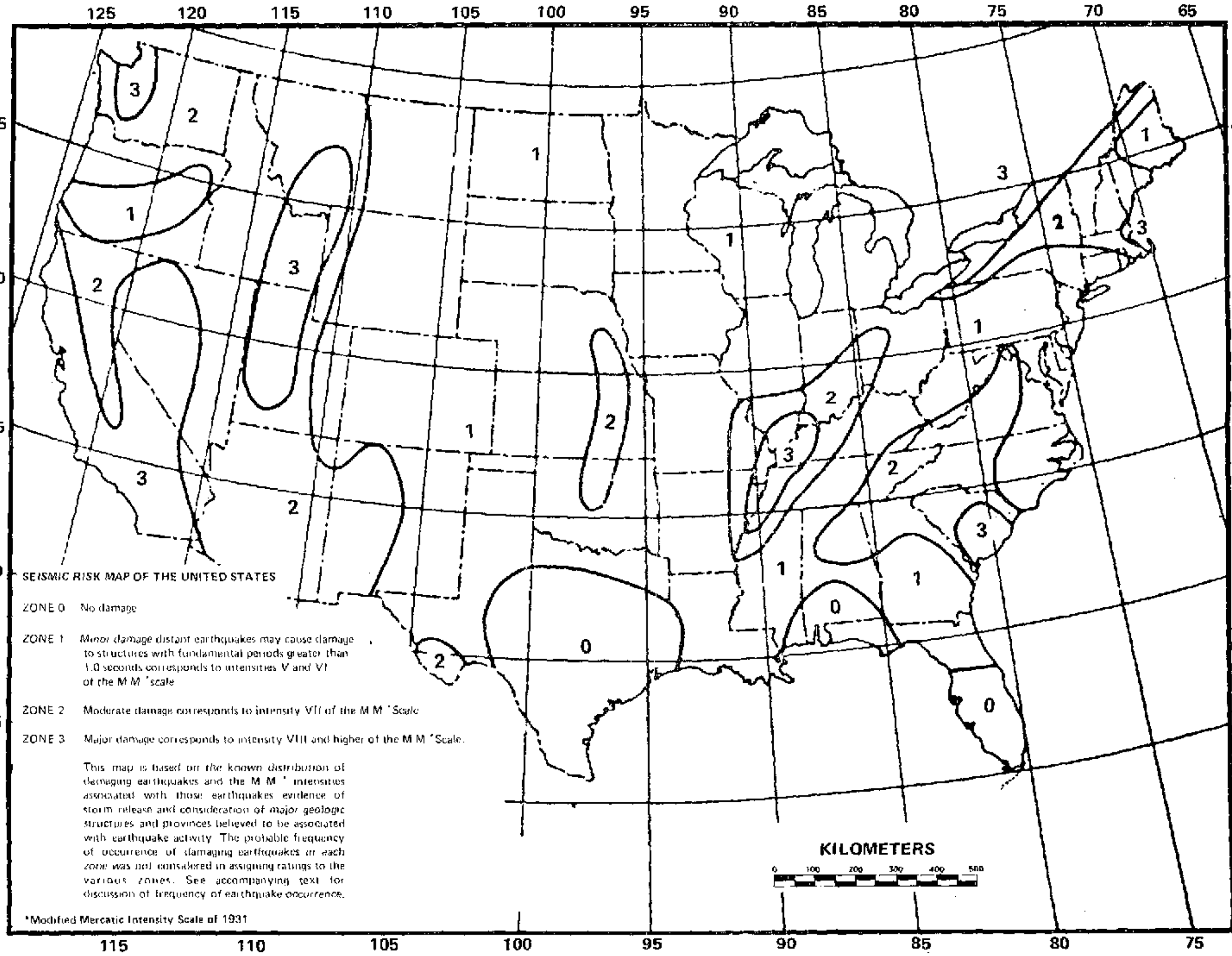

Figure 18. Seismic risk map of the United State. From "Seismic Risk Studies in the United State," by S. T. Algermissen, Fourth World Conference on Earthquake Engineering, vol. I, p. 26, 1969. Refs. 5, 27.

REFERENCES

1. Scholz, C., Sykes, L., & Aggarwal, Y., "The Physical Basis for Earthquake Prediction," AGU Meeting, Washington, April '73.

2. Whitcomb, J. H., Garmany, J. D., Anderson, D. L., "Earthquake Prediction: Variation of Seismic Velocities before the San Francisco Earthquake," SCIENCE, Vol. 180, pp. 632-635.

3. Kelleher, J., Sykes, L., and Oliver, J., "Possible Criteria for Predicting Earthquake Locations and Their Application to Major Plate Boundaries of the Pacific and the Caribbean," Journal of Geophysical Research, Vol. 78, No. 14, May 1973.

4. Sea level data were those corrected for oceanographic and meteorological conditions by Yamaguti, S., Bull. Earthquake Res. Inst. 46, 1269 (1968). Leveling data are from Tsubokawa, V., Dambara, T. and Okada, A., in Genl. Rept. on the Niigata Earthquake, Kawasumi, H., ed. (Tokyo Electrical Engin. Coll. Press, 1968) p. 129.

5. NASA Earth and Ocean Physics Applications Program, September, 1972.

6. Allen, C., "The tectonic environments of seismically active and inactive areas along the San Andreas fault system, Stanford Univ. Publ. Geol. Sci., 11, 70, 1968.

7. Scholz, C., P. Molnar, and T. Johnson, Detailed studies of frictional sliding of granite and implications for the earthquake mechanism, J. Geophys. Res., 77, 6392, 1972.

8. Savage, J., and R. Burford, Strain accumulation in California, Bull. Seismol. Soc. Amer., 60, 1877, 1970.

9. Savage, J., and R. Burford, Discussion of paper by C. H. Scholz and T. J. Fitch, 'Strain accumulation along the San Andreas fault,' J. Geophys. Res., 76, 6469, 1971.

10. Scholz, C. H., and T. J. Fitch, Strain accumulation along the San Andreas fault, J. Geophys. Res., 74, 6649, 1969.

11. Scholz, C. H., and T. J. Fitch, Strain and creep in central California, J. Geophys. Res., 75, 4447, 1970.

12. Scholz, C. H., and T. J. Fitch, Reply to 'Discussion of paper by C. H. Scholz and T. J. Fitch,' 'Strain accumulation along the San Andreas' by J. C. Savage and R. O. Burford, J. Geophys. Res., 76, 6480, 1971.

13. Nason, R., Investigation of fault creep slippage in northern and central California, Ph. D. thesis, 250 pp., Univ. of Calif., San Diego, 1971.

14. Wyss, M., and J. Brune, Regional variations of source properties in southern California estimated from the ratio of short-to long-period amplitudes, Bull. Seismol. Soc. Amer., 61, 1153, 1971.

15. Siry, Joseph W., "A Geopause Satellite System Concept," Space Science Reviews, 14, 2, 314-341, and Third International Symposium on the Use of Artificial Satellites for Geodesy, 1971.

16. Lundquist, C. A., and Veis, G., "Geodetic Parameters for a 1966 Smithsonian Institution Standard Earth," Smithsonian Astrophysical Observatory Special Report No. 200, 1966.

17. Guier, W. H., and Newton, R. R., "The Earth's Gravitational Field as Deduced from the Doppler Tracking of Five Satellites" Journal of Geophysical Research, Volume 70, No. 18, September 1965.

18. Martin, C. F., and Roy, N. A., "An Error Model for the SAO 1969 Standard Earth," Third International Symposium on the Use of Artificial Satellites for Geodesy, Sponsored by the AGU in cooperation with the AIAA, NOAA/NOS, and the U.S. Army Topographic Command, April, 1971.

19. "Precision Pointing Control System Design and Analysis," TRW Report No. 13900-6012-R0-01, NASA Contract No. NAS5-21111, 1 July 1972.

20. Kant, S., Private Communication, 1973.

21. Scholz, C., Private Communication, 1973.

22. Hopfield, H. S., "Tropospheric Range Error Parameters: Further Studies," APL/JHU Report CP 015, June 1972.

23. Vonbun, F. O., "Earth and Ocean Physics Applications Program (EOPAP)," presented at the XXIII International Astronautical Congress, October 8-14, 1972, Vienna, Austria.

24. Smith, D., Savage, J., Tocher, D., Scholz, C., "The San Andreas Fault Experiment," Transactions of the AGU, Vol. 53, Number 4, April 1972.

25. Plotkin, H., Johnson, T., & Minott, P., "Progress in Laser Ranging to Satellites: Achievements and Plans," presented at the COSPAR, IAG Symposium Athens, Greece, May 1973.

26. Barazangi, M., and Dorman, J., "World Seismicity Maps of ESSA, Coast and Geodetic Survey Epicenter Data for 1961-1967," Bull. Seismol. Soc. Amer., 59, 369, 1969.

27. Algermissen, S. T., "Seismic Risk Studies in the United States," Fourth World Conference on Earthquake Engineering, Vol. I, p. 26, 1969.

NASA–GSFC